



Interleukin-6 gene transfer reverses body weight gain and fatty liver in obese mice



Yongjie Ma, Mingming Gao, Hao Sun, Dexi Liu*

Department of Pharmaceutical and Biomedical Sciences, College of Pharmacy, University of Georgia, GA 30602, USA

ARTICLE INFO

Article history:

Received 9 October 2014

Received in revised form 16 January 2015

Accepted 21 January 2015

Available online 4 February 2015

Keywords:

IL-6

Obesity

Weight loss

Insulin resistance

Energy expenditure

ABSTRACT

Interleukin-6 (IL-6) is a multifunctional protein and has a major influence on energy metabolism. The current study was designed to assess the therapeutic effect of overexpression of *Il-6* gene through gene transfer on high fat diet-induced obese mice. Hydrodynamic delivery of 1 μ g pLIVE-IL6 plasmid per mouse into C57BL/6 obese mice resulted in peak level at 10 ng/ml of circulating IL-6 1 day after gene transfer and above 1 ng/ml thereafter for a period of 6 weeks. Persistent *Il-6* gene expression did not affect food intake but induced a significant reduction in body weight and improved obesity-associated hepatic steatosis. *Il-6* gene delivery enhanced thermogenic gene expression and elevated protein levels of phosphorylated STAT3, PGC1 α and UCP1 in brown adipose tissue. *Il-6* overexpression elevated mRNA levels of lipolysis genes, triggered phosphorylation of STAT3, AMPK, and ACC, and increased expression of genes involved in fatty acid oxidation in skeletal muscle. IL-6 did not affect macrophage infiltration but maintained the M2 macrophage population in adipose tissue. Collectively, these results suggest that overexpression of the *Il-6* gene by hydrodynamic gene delivery induces weight loss and alleviates obesity-induced fatty liver and insulin resistance, supporting the notion that gene transfer is a valid approach in managing obesity epidemics.

© 2015 Elsevier B.V. All rights reserved.

1. Introduction

Interleukin-6 (IL-6), produced by immune and non-immune cells, is a multifunctional cytokine. IL-6 is commonly known as a pro-inflammatory cytokine that regulates immunoreaction and acute immune response. More recent studies have shown that IL-6 has an anti-inflammatory activity as it increases the production of IL-10, IL-1 receptor antagonist (IL-1ra), and soluble TNF-receptors [1–3]. In addition to modulating the immune system, IL-6 has also attracted particular attention for its pivotal role in regulating energy expenditure, body composition and peripheral lipid metabolism [4–6].

The effects of IL-6 on nutrient homeostasis and obesity remain controversial and unresolved. IL-6 is generally considered an obesity-related inflammatory factor and mediator for insulin resistance as elevated circulating IL-6 is correlated with adiposity and insulin resistance in humans [7–9]. However, substantial evidence suggests that IL-6 exerts a beneficial influence in this context. Physical exercise promotes secretion of IL-6 from skeletal muscle and the blood concentration of IL-6 increases about 100-fold, improving insulin sensitivity

[10,11], while IL-6 knockout mice developed obesity, systemic insulin resistance and inflammation [4,12], which could be partially reversed by intra-cerebriventricular injection of the IL-6 protein [4]. Meanwhile, direct delivery of adeno-associated viral vectors containing the *Il-6* gene into the rat hypothalamus or mice carrying the human *Il-6* gene suppressed weight gain and visceral adiposity [13,14], indicating that IL-6 exerts anti-obesity effects in rodents. Moreover, short-term intra-cerebroventricular injections of the recombinant IL-6 protein and a peripheral increase in *Il-6* gene expression induced weight loss and improved insulin sensitivity in mice [15,16]. Although these studies support the potential application of IL-6 in fighting obesity, the systemic effects of prolonged elevation of IL-6 level in obese mice remain unknown.

Here we preserve sustained *Il-6* expression in obese mice by hydrodynamic gene delivery and demonstrate that long-term maintenance of IL-6 levels significantly induced weight loss in obese mice by enhancing lipolysis and energy metabolism, resulting in improved insulin sensitivity and maintenance of glucose homeostasis as well as a reduction in fat accumulation in the liver. *Il-6* gene transfer did not affect macrophage infiltration, but countered the obesity-related inflammatory signal by enhancing the expression of M2 macrophage gene markers and related anti-inflammatory factor genes. Our results indicate the long-term beneficial effects of IL-6 elevation on obesity and suggest the potential application of *Il-6* gene transfer as a means of controlling obesity and obesity-related metabolic disorders.

* Corresponding author at: Department of Pharmaceutical and Biomedical Science, University of Georgia College of Pharmacy, 450 Pharmacy South, 250 West Green Street, Athens, GA 30602, USA. Tel.: +1 706 542 7385; fax: +1 706 542 5358.

E-mail address: dliu@uga.edu (D. Liu).

2. Methods and materials

2.1. Plasmid construction

A mouse *Il-6* open reading fragment was obtained from OriGene (Rockville, MD) and reconstructed into a pLIVE plasmid vector (Mirus Bio, Madison, WI) at the *NheI* and *XhoI* cutting sites. The insertion in the new plasmid (pLIVE-IL6) was confirmed using DNA sequencing. The pLIVE-IL6 and empty plasmids were purified using CsCl-ethidium bromide density-gradient ultracentrifugation and kept in saline (0.9% sodium chloride). Purity of the plasmids was verified with absorbency ratio at 260 and 280 nm and by 1% agarose gel electrophoresis.

2.2. Animal treatment

C57BL/6 mice (male, 10-week old) were purchased from Charles River Laboratories (Wilmington, MA) and housed under standard conditions with a 12 h light–dark cycle. All procedures performed on animals were approved by the Institutional Animal Care and Use Committee at the University of Georgia, Athens, Georgia. Obese mice (50 ± 2 g) were developed by feeding animals for 20 weeks with high fat diet (HFD) (60% kJ/fat, 20% kJ/carbohydrate, 20% kJ/protein, Bio-Serv, Frenchtown, NJ). Regular mice were fed with a standard laboratory chow diet (20% kJ/fat, 60% kJ/carbohydrate, 20% kJ/protein, LabDiet, St Louis, MO). Food consumption was determined by measuring the difference between the amount provided and the amount left every three days. Food intake per mouse was calculated based on the amount consumed divided by time and the number of mice per cage. The procedure for hydrodynamic gene delivery in obese mice was performed according to an established procedure [17,18] with some modification. Briefly, an appropriate volume of saline solution (equivalent to 8% lean mass of an obese mouse) containing 1 µg pLIVE-IL6 or empty plasmid was injected through the tail vein within 5–8 s. Mice were continually fed an HFD for 6 weeks. The body weight of each mouse was measured on an electronic balance, and body composition was analyzed using EchoMRI-100 (Echo Medical Systems, Houston, TX) once per week. The same procedures were also performed on age-matched male mice with chow feeding. Blood was collected at the desired time points using a Microvette-CB300-LH from Fisher Scientific (Pittsburgh, PA) and plasma *Il-6* concentrations were determined using ELISA kits from eBioscience (San Diego, CA). Rectal temperature of the mice at desirable time points was measured using a specially designed Thermocouple Meter from Kent Scientific Corp (Torrington, CT).

2.3. Evaluation of glucose homeostasis and insulin sensitivity

Insulin concentrations were determined using a Mercodia Insulin ELISA kit from Mercodia Developing Diagnostics (Winston Salem, NC) following the provided protocol. For the glucose tolerance test (GTT), mice were injected intraperitoneally with glucose at 1.5 g/kg body weight after 6 h fasting. Blood samples were taken at varying time points and glucose concentrations were determined using glucose test strips and TUREtrack glucose meters from Nipro Diagnostics Inc. (Fort Lauderdale, FL). For the insulin tolerance test (ITT), mice fasted for 4 h and blood glucose levels were measured after an intraperitoneal injection of insulin (0.75 U/kg) from Eli Lilly (Indianapolis, IN). HOMA-IR values were calculated based on the formula: (fasting insulin [µU/ml] × fasting glucose [mmol/l])/22.5.

2.4. Histochemical and Oil Red O analysis

After mice were sacrificed, the liver, WAT, and BAT were collected, fixed in 10% formalin and embedded in paraffin. Hematoxylin and eosin (H&E) staining was performed using tissue sections at a thickness of 6 µm. Frozen liver sections (8 µm) were stained with 0.2% Oil Red O reagent (Electron Microscopy Sciences, Hatfield, PA) in 60% isopropanol

for 15 min, washed three times with phosphate buffered saline and counter-stained with hematoxylin for 1 min. A microscopic examination was performed and photographs were taken under a regular light microscope.

2.5. Blood and hepatic lipid analysis

A quantitative determination of liver lipids was performed following an established procedure [19,20]. Briefly, liver tissues (100–200 mg) were homogenized in phosphate buffered saline (1 ml), mixed with 5 ml of organic solvent (chloroform: methanol = 2:1, vol/vol) and incubated overnight at 4 °C. The mixture was centrifuged and the organic phase collected. The collected fraction was dried and lipids were re-dissolved in 1% Triton X-100. The amounts of cholesterol, triglyceride (Thermo Fisher Scientific Inc., Waltham, MA) and free fatty acids (Wako Bioproducts, Richmond, VA) were determined following the manufacturers' instructions. The same kits were also used for blood lipid analysis.

2.6. Gene expression analysis by real time PCR

Total RNA was isolated from mouse livers, the pancreas, WAT and BAT using the TRIZOL reagent (Life Technologies, Grand Island, NY) or RNeasy Lipid Tissue Mini Kit (QIAGEN, Valencia, CA) according to the

Table 1
Primer sets for real time PCR analysis of gene expression.

Name	Forward sequence	Reverse sequence
<i>Pparγ1</i>	GGAGACCACTCGCATTCTT	GTAATCAGCAACCATTGGGTCA
<i>Pparγ2</i>	TCGCTGATGCACTGCCTATG	GAGAGGTCCACAGAGCTGATT
<i>Cd36</i>	CCTAAAGGAATCCCCGTGT	TGCATTTGCCAATGTCTAGC
<i>Fabp4</i>	AAGGTGAAGAGCATCATAACCC	TCACGCCCTTCATAACACATTC
<i>Mgat1</i>	TGGTGCCAGTTTGGTTCCAG	TGCTCTGAGTCCGGTTCA
<i>Pparα</i>	TGTCGAATATGTGGGACAA	AATCTTGACGTCGGATCAC
<i>Acox1</i>	CCGCAACCTCAATCCAGAG	CAAGTTCTCGATTCTCGACGG
<i>Cpt1a</i>	CTCCGCTGAGCCATGAAG	CACCAGTATGATGCCATCT
<i>Cpt1b</i>	GGTCTCTTCTCAAGGTCTG	CGAGGATCTCTGGAAGTGC
<i>Srebp-1c</i>	CCCTGTGTACTGGCCTTT	TTGCCATGTCTCCAGAAGTG
<i>Acc-1</i>	GCCTCTTCTGACAAACGAG	TGACTGCCGAAACATCTCTG
<i>Fas</i>	AGAGATCCCGAGACGCTTCT	CCCTGGTAGGCAATCTGTAGT
<i>Scd-1</i>	TTCTTACAGACCACCACCA	CCGAGAGGCGAGGTGTAGAG
<i>Cyp7a1</i>	AACGGGTGATTCACATACCTGG	GTGGACATATTTCCCATCAGTT
<i>Hmgcr</i>	CTTGTGGAATGCCCTTGTGATTG	AGCCGAAGCAGACATGAT
<i>Pepck</i>	AAGCATTCAACGCCAGGTTC	GGGCGAGTCTGTCAGTTCAAT
<i>G6pase</i>	CGACTCGCTATCTCCAAGTGA	GTTGAAACAGTCTCCGACCA
<i>Insulin1</i>	CACCTCTACCCCTGTG	ACCACAAAGATGCTGTTTGACA
<i>Insulin2</i>	GCTTCTTACACACCCATGTG	AGCACTGATCTCAACATGCCAC
<i>Hsl</i>	GCTTGGTTCAACTGGAGAGC	GCCTAGTCCCTTCTGGTCTG
<i>Atgl</i>	CAACGCCACTCACATCTACCG	TCACCAGGTTGAAGGAGGGAT
<i>Ucp1</i>	AGGCTTCCAGTACCAATTAGT	CTGCTGAGCCCTTGGTGTAG
<i>Ucp2</i>	GCGTCTGGGTACCATCTA	GCGTATCATGCTTGAAT
<i>Ucp3</i>	ATGAGTGTGCTCCATTCC	GGCGTATCATGCTTGAAT
<i>Pgc-1α</i>	GAAGTGGGTAGCGACCAATC	AATGAGGGCAATCCGTCTTCA
<i>Pgc-1β</i>	TTGTAGAGTGCCAGGTGCTG	GATGAGGGAAAGGACTCCTC
<i>Dio2</i>	AATTATGCTCGGAGAAGACCG	GGCAGTTGCTAGTGAAGGT
<i>Cidea</i>	ATCACAACCTGGCCTGGTTACG	TACTACCCGGTGTCCATTTCT
<i>Elovl3</i>	TTCTCAGCCGGTTAAAATGG	GAGCAACAGATAGACGACCAC
<i>F4/80</i>	CCCCAGTGTCTTACAGAGTG	GTGCCAGAGTGGATGTCT
<i>Cd68</i>	CCATCCTTACAGATGACACCT	GGCAGGGTATGAGTGACAGTT
<i>Cd11b</i>	ATGGACGCTGATGGCAATACC	TCCCAATTCACGCTCTCCCA
<i>Cd11c</i>	ACGTCAGTACAAGGAGATGTTGGA	ATCCTATTGCAAGATGCTTCTTACC
<i>Mcp-1</i>	ACTGAAGCCAGCTCTCTTCTCTC	TTCTTCTTGGGGTACGACAGAC
<i>Tnfα</i>	CCCTCACACTCAGATCATCTTCT	GCTACGAGCTGGGCTACAG
<i>Il-1β</i>	GCAACTGTTCTGAACTCAACT	ATCTTTTGGGTCCTCAACT
<i>Cd163</i>	TCCACAGTCCAGAACAGTC	CCTTGGAAACAGAGACAGGC
<i>Cd206</i>	CAGGTGTGGCTCAGGTAGT	TGTGGTGAAGTGAAGGTTGA
<i>Il-10</i>	GCTCTTACTGACTGGCATGAG	CCGAGCTTAGGAGCATGTG
<i>Il-4</i>	GGTCAACCCAGCTAGT	CCGATGATCTCTCTCAAGTGT
<i>Il-4α</i>	TCTGCATCCCTGTTTTCG	GCACCTGTGATCTGAAATG
<i>Il-13</i>	CCTGGCTTGTGCTGCCTT	GGTCTTGTGATGTGCTCA
<i>Il-13α1</i>	TCAGCCACCTGTGACGAATTT	TGAGGTGCAATTTGGACTGG
<i>Acadl</i>	TCTTTTCTCGGAGCATGACA	CAGACCTCTACTCACTTCCAG
<i>Gapdh</i>	AGTCCGGTGAACGGATTTG	TGTAGACCATGTAGTTGAGGTCA

manufacturers' protocols. One microgram of total RNA was employed for the first strand cDNA synthesis using a First-strand cDNA Synthesis System from OriGene (Rockville, MD). Real time PCR was performed in an ABI StepOne Plus Real Time PCR system (Foster City, CA) using PerfeCTa® SYBR® Green FastMix (Quanta BioSciences, Gaithersburg, MD) as the indicator. PCR was carried out for 40 cycles at 95 °C for 15 s and 60 °C for 1 min. The data were analyzed using the $\Delta\Delta C_t$ method and normalized to internal control of GAPDH mRNA. Primers were synthesized at Sigma (St. Louis, MO). All primer sequences employed are summarized in Table 1. Melting curve analysis of all real-time PCR products was conducted and showed a single DNA duplex.

2.7. Western Blotting analysis

Tissue samples were homogenized on ice using a Tissue Tearor in 1 ml lysis buffer (25 mM Tris-HCl, 150 mM NaCl, 1% NP-40, 1% sodium deoxycholate, 0.1% SDS, pH 7.6) with a protease inhibitor cocktail from Millipore (Billerica, MA). The tissue homogenates were centrifuged at 12,000 rpm for 10 min and total proteins were extracted from the supernatant. Fifty micrograms of proteins was separated on a 7.5% SDS-polyacrylamide gel and transferred onto a polyvinylidene difluoride membrane using a Bio-Rad Mini-Blot transfer apparatus (Richmond, CA). Membranes were blocked in a Tris-buffered solution containing 5% non-fat milk for 1 h. Immunoblotting was performed at 4 °C overnight with shaking using antibodies against UCP1, PGC1 α from Abcam (Cambridge, MA), STAT3, p-STAT3, AMPK, p-AMPK, ACC, p-ACC from Cell Signaling (Boston, MA) or GAPDH from Santa Cruz Biotechnology (Santa Cruz, CA), respectively. After washing, the membranes were incubated in a 1:3000 dilution of a secondary antibody at room temperature for 1 h in Tris-buffered solution containing 0.5% of Tween-20. Protein bands were visualized using Pierce ECL Western Blotting substrate (Rockford, IL).

2.8. Statistical analysis

A statistical analysis was performed using the Student's *t* test. All data are reported as mean \pm standard deviation (SD) with statistical significance set at *P* < 0.05.

3. Results

3.1. Prolonged *Il-6* gene expression induces weight loss in C57BL/6 obese mice

The level and time-dependent *Il-6* gene expression after hydrodynamic delivery of 1 μ g of pLIVE-IL6 plasmids was examined in obese mice fed an HFD. Results in Fig. 1A show that blood concentration of IL-6 protein reached the peak level (~10 ng/ml) 1 day after gene transfer and declined slightly with time. Six weeks after gene transfer, circulating IL-6 level remained at approximately 1 ng/ml, 50-fold higher than that of control mice (~20 pg/ml) injected with empty plasmid. PCR analysis revealed the highest level of *Il-6* gene expression in the liver, 120-fold higher than the background level in control animals (Fig. 1B). A slight increase of mRNA level was also seen in BAT and skeletal muscle. Blood chemistry tests showed no increase of serum concentrations of AST and ALT in animals with *Il-6* gene transfer at the end of 6-week experiment (Fig. 1C). These results prove that *Il-6* gene expression can be successfully achieved and sustained after hydrodynamic gene delivery.

The therapeutic effect of prolonged *Il-6* gene expression on obese mice is shown in Fig. 1D and E. A slight decrease in body weight was seen immediately after plasmid injection in both treated and control animals due to effect of the procedure. However, animals injected with pLIVE-IL6 plasmid continued to lose weight and eventually reached a steady state with an average body weight of 38 g in 6 weeks, losing an average of 12 g of their initial body weight of 50 \pm 2 g. In contrast, control mice regained the body weight initially lost and gained an additional 2 g by the end of the experiment. The analysis of body composition by magnetic resonance imaging (MRI) revealed that weight loss in animals with *Il-6* gene transfer is fully correlated to the time-dependent decrease in fat mass (Fig. 1F), not lean mass (Fig. 1G). No change in fat and lean mass was observed in control animals. Moreover, the loss of body weight is not correlated to food intake (Fig. 1H). In addition, body fat reduction was further determined by weighing fat pads. Results in Fig. 2A and B show that *Il-6* gene transfer significantly reduced the size of fat pads including subcutaneous (subWAT), epididymal (epiWAT) and retroperitoneal (retroWAT) adipose tissues in obese

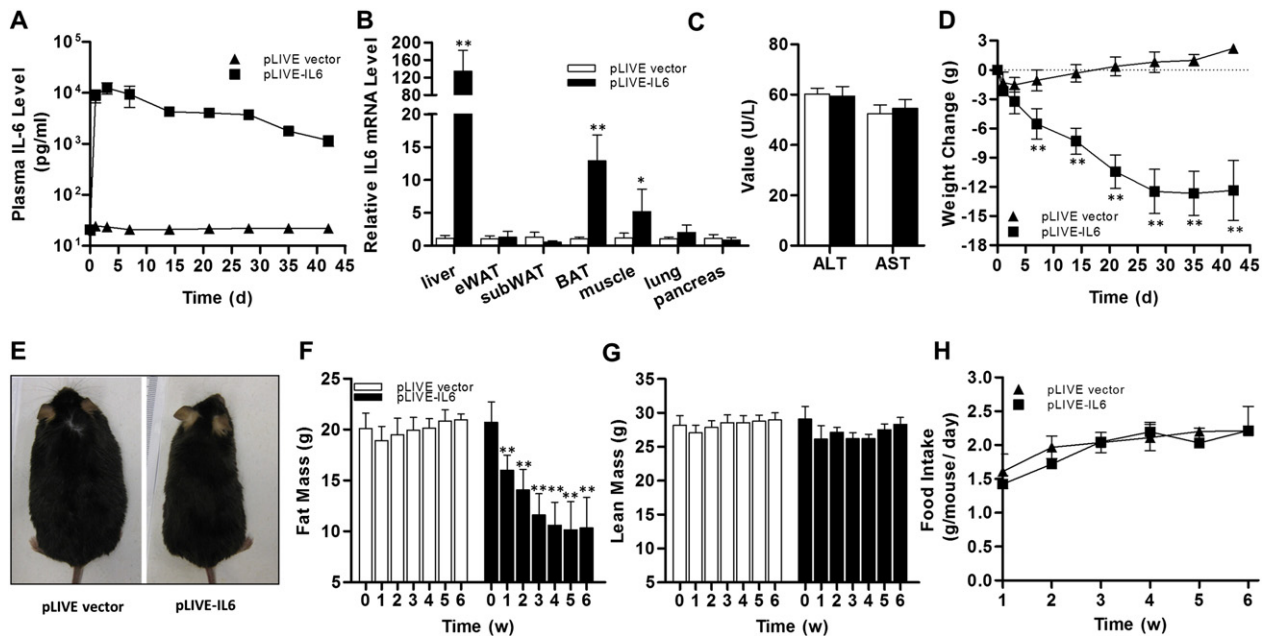


Fig. 1. Effects of hydrodynamic *Il-6* gene transfer on C57BL/6 obese mice. C57BL/6 obese mice (male, 50 \pm 2 g) were hydrodynamically injected via tail vein of 1 μ g of pLIVE-IL6 or pLIVE empty plasmid DNA. (A) Circulating IL-6 levels as a function of time; (B) *Il-6* mRNA level in different tissues 6 weeks after gene transfer; (C) Plasma AST and ALT levels at the end of 6-week *Il-6* gene expression; (D) Weight change in obese mice; (E) Representative images of mice at the end of the experiment; (F, G) Body composition of fat mass and lean mass at different times; and (H) Food intake. Results represent mean \pm SD (n = 10) for each group. **P* < 0.05, ***P* < 0.01, comparing to control mice injected with pLIVE empty plasmid.

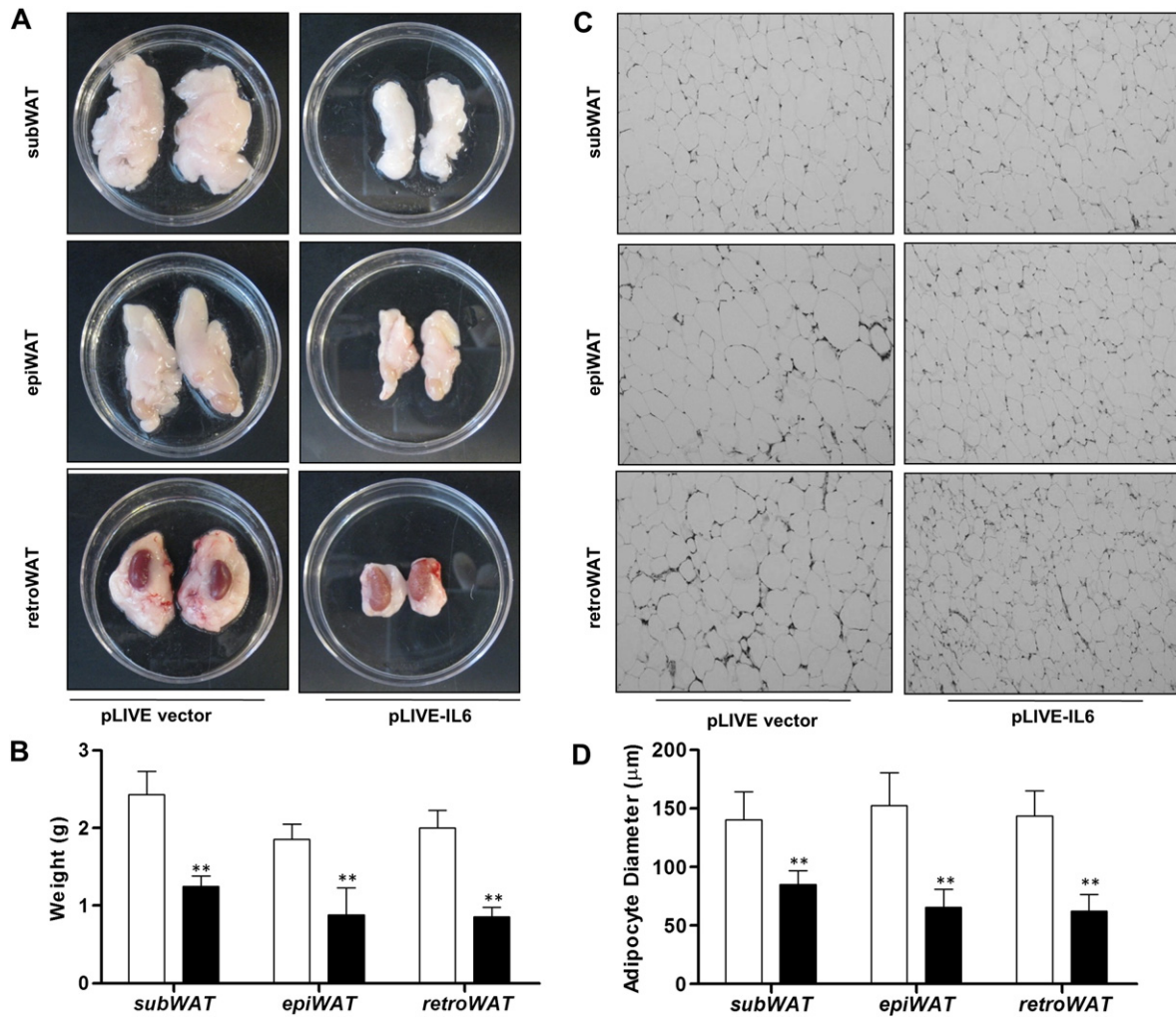


Fig. 2. IL-6 reduced fat tissues depots and the size of adipocytes in obese mice. Obese mice were sacrificed at the end of the 6-week after gene transfer and different fat pads were collected and weight determined. Tissues were fixed in 10% neutral buffered formalin. H&E staining was performed to show the morphology of adipose tissues. (A) Appearance of subcutaneous (subWAT), epididymal (epiWAT) and retroperitoneal (retroWAT) fat tissues collected from obese mice; (B) Weight of fat pads in (A); (C) Representative images of H&E staining of subWAT, epiWAT and retroWAT (100 \times); and (D) Average diameter of adipocytes in different fat pads (calculated from 200 adipocytes from 4 separate slides). Results represent mean \pm SD. * $P < 0.05$, ** $P < 0.01$, comparing to control obese mice injected with pLIVE empty plasmid.

mice by ~ 0.9 , ~ 1.2 and ~ 1.0 g, respectively. Accordingly, H&E staining of adipocytes in subWAT, epiWAT and retroWAT showed reduced size of adipocytes (Fig. 2C), which was also confirmed by quantification analysis using an imaging system (Fig. 2D).

To examine whether IL-6 gene transfer only affects fat mass, we performed the same set of experiments in age-matched chow-fed mice. The expression of IL-6 gene after hydrodynamic gene delivery slightly reduced body weight of normal mice by 2.5 g due to reduced fat mass, but not lean mass (Fig. 3A, C and D). Again, IL-6 gene transfer did not affect food intake in mice fed a regular chow (Fig. 3B). Taken together, these data demonstrate that prolonged IL-6 gene expression reduces body weight and fat mass without affecting food intake.

3.2. Sustained IL-6 level alleviates hepatic steatosis in obese mice

Obese mice displayed an extensive vacuolation in H&E stained liver section (Fig. 4A), indicating severe fat accumulation in the liver. IL-6 gene transfer dramatically reduced fat accumulation in the liver, as evidenced by the recovered normal liver structure (Fig. 4A) and fewer lipid droplets stained by Oil Red O (Fig. 4B). Consistent with these results, IL-6 gene transfer significantly

reduced hepatic triglyceride, total cholesterol and free fatty acid levels in obese animals (Fig. 4C–E). IL-6 gene transfer also reduced blood concentrations of free fatty acid, but not triglyceride levels (Fig. 4F–H).

A real time PCR analysis was carried out to evaluate the effect of IL-6 gene transfer on the expression of genes involved in hepatic fat accumulation. Fig. 5A shows that IL-6 gene transfer markedly suppressed mRNA levels of peroxisome proliferator-activated receptor gamma (*Ppar γ 1*) (42%), *Ppar γ 2* (83%), and their target genes, including *Cd36* (71%), fatty acid binding protein 4 (*Fabp4*, 46%), and monoacylglycerol O-acyltransferase 1 (*Mgat1*, 99%). At the end of the 6-week experiment, IL-6 did not affect *Ppar α* and its target genes including carnitine palmitoyl-transferase 1 (*Cpt1*) and peroxisomal acyl-coenzyme A oxidase 1 (*Acox1*) (Fig. 5B). IL-6 also did not significantly affect hepatic lipogenic genes with the exception of reducing fatty acid synthase (*Fas*) gene expression by 46%. In regard to cholesterol metabolism, IL-6 enhanced 3-hydroxy-3-methylglutaryl coenzyme A reductase (*Hmgcr*) gene expression by 2 fold and increased cholesterol 7 α -hydroxylase (*Cyp7a1*) gene expression by 4.3 fold (Fig. 5C). Collectively, these data demonstrate that prolonged IL-6 gene expression alleviates obesity-associated fatty liver.

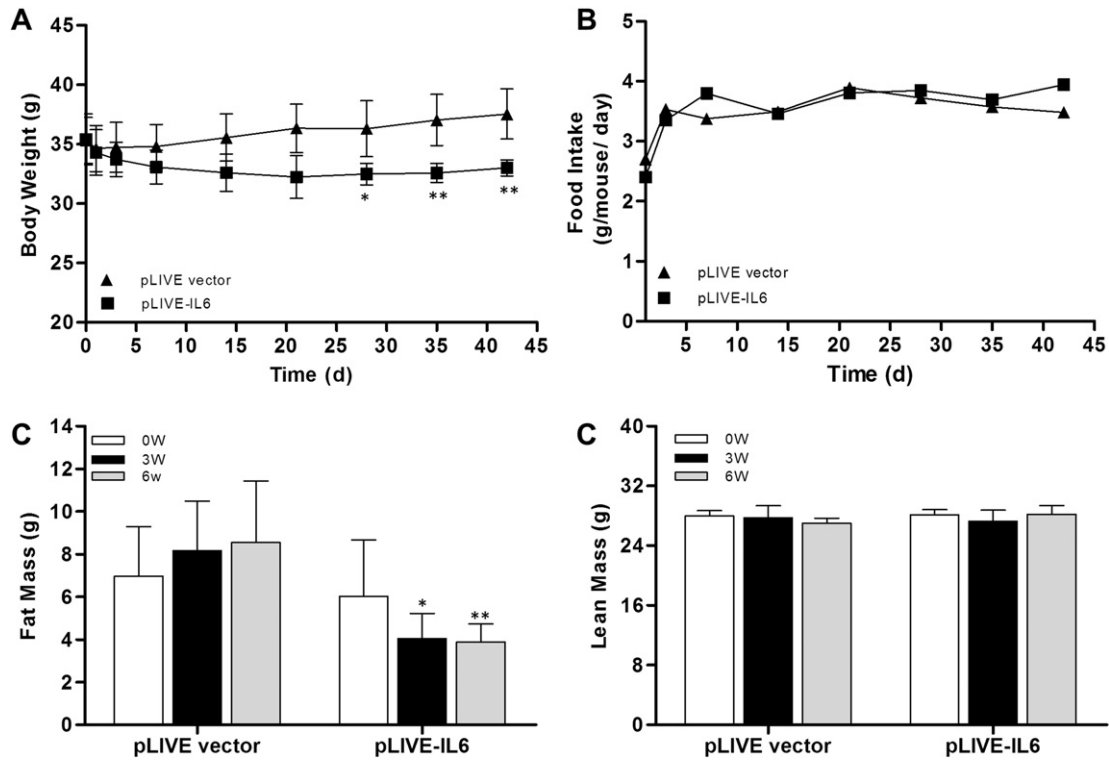


Fig. 3. Elevation of *Il-6* gene expression in age-matched chow-fed C57BL/6 mice decreased the fat mass. One microgram of pLIVE-IL6 or pLIVE empty plasmid was delivered to each chow-fed C57BL/6 male mouse through a hydrodynamic-based procedure. (A) Growth curve; (B) Food intake; and (C, D) Fat mass and lean mass at different times. Results represent mean \pm SD ($n = 5$) for each group. * $P < 0.05$, ** $P < 0.01$, comparing to control mice injected with pLIVE empty plasmid.

3.3. Elevation of *IL-6* level improves insulin sensitivity and glucose homeostasis in obese mice

To address the impact of *Il-6* gene transfer on insulin sensitivity and glucose homeostasis, we monitored blood insulin levels and pancreatic insulin gene expression. *IL-6* dramatically suppressed obesity-induced hyperinsulinemia by 78% (Fig. 6D). Accordingly, pancreatic mRNA levels of *Insulin1* and *Insulin2* genes were markedly lower in mice with *Il-6* gene transfer compared to control obese animals (Fig. 6E, F). In the meantime, a glucose tolerance test (Fig. 6A) and calculated area under the curve (AUC, Fig. 6B) revealed a lower peak level and much higher clearance rate of intra-peritoneally injected glucose in animals with *Il-6* gene transfer. Moreover, mice with *Il-6* gene transfer were more sensitive to insulin than control obese mice when tested using an insulin tolerance test (Fig. 6C), and improved insulin sensitivity was also reflected by reduction in calculated HOMA-IR (Fig. 6G), the assessment index of insulin resistance. Taken together, these data indicate that *Il-6* gene transfer improves insulin sensitivity and glucose homeostasis in obese mice.

3.4. *IL-6* treatment enhances lipolysis and stimulates thermogenesis in obese mice

IL-6 has been shown to increase energy expenditure by stimulating the function of brown adipose tissue (BAT) [13,21]. Result in Fig. S1 shows that *IL-6* increased the body temperature by 0.8 °C 1 day after gene transfer followed by a gradual decline thereafter, suggesting enhanced energy expenditure. H&E stained BAT showed a dramatic reduction in lipid droplets and the density of vacuole type structures (Fig. 7A). Data in Fig. 7B show that *IL-6* increased the expression of genes involved in lipid utilization and thermogenesis in BAT including the fatty acid transporter gene (*Cd36*, ~1.6-fold), hormone-sensitive lipase

(*Hsl*, ~2.2-fold), and adipose triglyceride lipase (*Atgl*, ~5.4-fold). *IL-6* also elevated the expression of genes responsible for fatty acid oxidation (*Cpt1*, ~2.0-fold) and thermogenesis in BAT, as reflected by increased thermogenic genes including *Ucp1* (~1.9-fold), *Ucp2* (~1.6-fold), *Ucp3* (~4.8-fold), *Pgc1* (~2.0-fold), *Cidea* (~2.6-fold), and *Elovl3* (~3.5-fold). Moreover, a Western Blotting analysis (Fig. 7C) confirmed that *IL-6* significantly activated its signaling molecule of STAT3 in BAT, as evidenced by a 3-fold increase in the ratio of the p-STAT3 to STAT3 (Fig. 7D). Consequently, higher *IL-6* levels enhanced protein levels of PGC1 α and UCP1, two key effectors in thermogenesis (Fig. 7E). In addition, *Il-6* gene transfer increased the expression of *Hsl*, *Atg*, *Cpt1* in subcutaneous WAT (Fig. 8A–B).

Skeletal muscle is another tissue capable of utilizing fatty acids. As shown in Fig. 9A and B, *IL-6* stimulated phosphorylation of STAT3 in skeletal muscle by 1.6-fold, indicating its potential function in muscle. We found that *IL-6* stimulated the phosphorylation of AMPK, a master regulator for fatty acid oxidation [22], and its downstream target acetyl-CoA carboxylase (ACC) in skeletal muscle (Fig. 9A, C and D). Results shown in Fig. S2 demonstrate that mRNA levels of peroxisomal acyl-coenzyme A oxidase 1 (*Acox1*), *Cpt1a*, *Cpt1b* and long-chain specific acyl-CoA dehydrogenase (*Acadl*) gene were significantly increased in animals with *Il-6* gene transfer. In the meantime, the mRNA levels of *Ucp3* and *Pgc1 α* were also elevated by ~2.0-fold and ~3.0-fold, respectively, suggesting that *IL-6* has enhanced lipid utilization in skeletal muscle.

3.5. Sustained *IL-6* treatment did not affect macrophage infiltration, but increased the M2 macrophage population in adipose tissue and liver

Finally, we examined the effect of *Il-6* gene transfer on macrophage infiltration and inflammatory response in BAT, WAT and liver tissue (Fig. 10). *IL-6* did not reduce existing macrophages, although it did dramatically reduce chemo-attractant *Mcp-1* gene expression in all tested

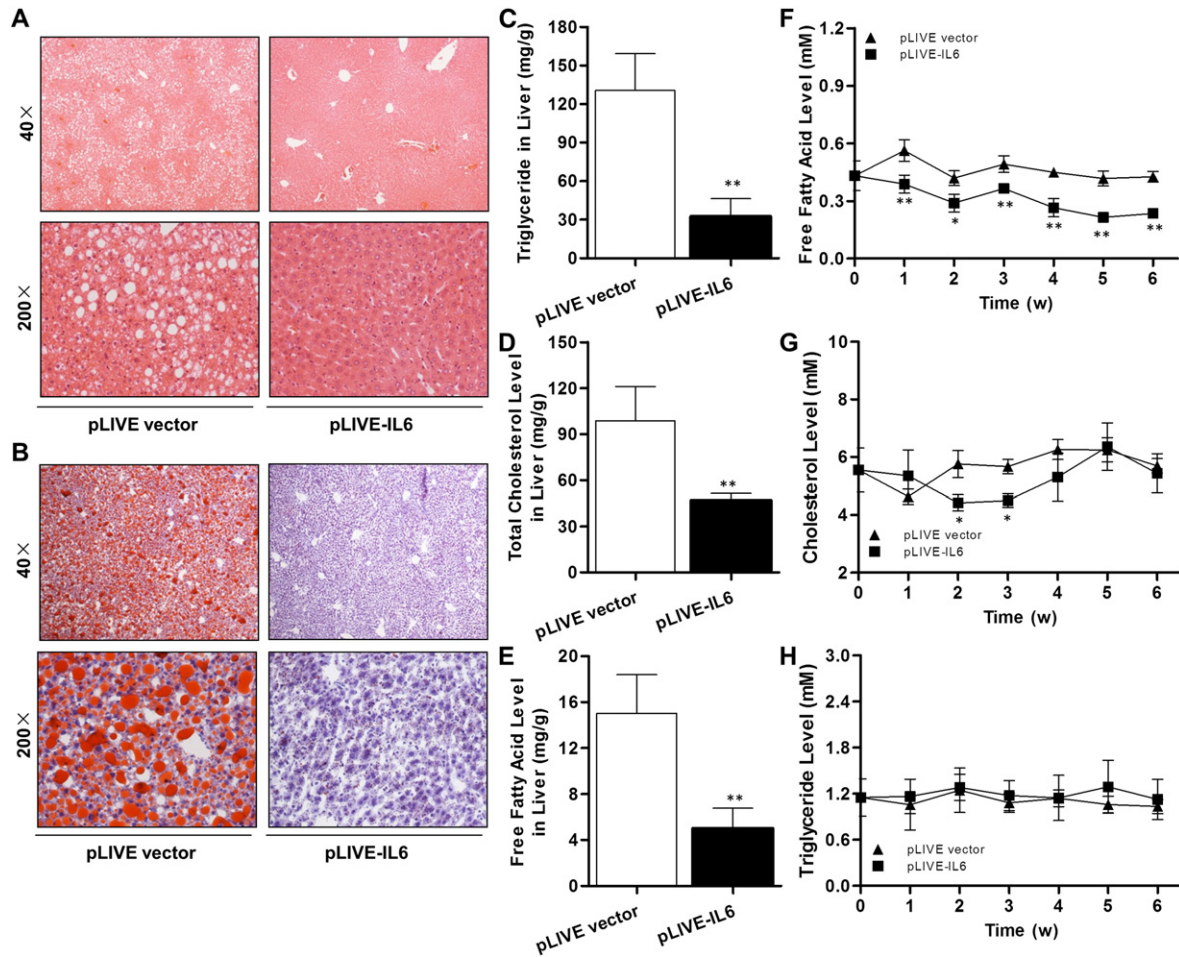


Fig. 4. IL-6 improves obesity-induced fatty liver. Mice were sacrificed at the end of 6 weeks after hydrodynamic gene transfer and livers were collected. (A) Image of liver structure by H&E staining; (B) Images of liver sections stained for lipid distribution with red oil O staining; (C–E) Triglyceride, free fatty acid and total cholesterol contents in the liver; and (F–H) Serum concentrations of triglyceride, free fatty acid and cholesterol 6 weeks after gene transfer. Each data point represents the mean \pm SD of 6 animals in each group. * $P < 0.05$, ** $P < 0.01$ compared to control group.

tissues. However, *Il-6* gene transfer significantly increased expression of M2 macrophage marker genes such as *Cd163* and *Cd206* in BAT, subWAT and the liver. In the meantime, IL-6 evidently enhanced the transcript levels of anti-inflammatory *Il-10* and M2-related factor *Il-4*, *Il-13* and their receptors. Taken together, these results suggest that IL-6 counterbalances obesity-associated pro-inflammation by increasing M2 macrophage population and the level of anti-inflammatory factors.

4. Discussion

In the current study, we examined the long-term effects of *Il-6* gene transfer on obesity and related metabolic syndromes and explored the potential molecular mechanisms. Our results show that sustained *Il-6* gene expression can be achieved in obese mice via the method of hydrodynamic gene delivery, resulting in reduction of body weight and fat mass (Figs. 1 and 2), alleviation of hepatic steatosis (Fig. 4), and improvement of glucose homeostasis (Fig. 6). These beneficial effects were associated with elevated lipid mobilization in WAT and enhanced thermogenesis in BAT (Figs. 7, 8). IL-6 did not reduce obesity-related macrophage infiltration, but significantly increased expression of M2 macrophage markers and anti-inflammatory factor genes (Fig. 10).

Reduction in body weight by hydrodynamic *Il-6* gene transfer is not caused by reduction in food intake (Fig. 1H). This conclusion is in agreement with previous study where adeno-associated viral vector was used to deliver the *Il-6* gene into the hypothalamus in rats [13]. It was

shown that AAV-mediated *Il-6* gene transfer suppressed weight gain of animals and the visceral adiposity but did not affect food intake in a period of 5 weeks. However, intracerebroventricular injection of recombinant IL-6 protein at 0.4 μ g/day resulted in reduction in food intake per body weight [15] but not at 100–200 ng level [4], suggesting critical impact of IL-6 dose on animal appetite.

Slight, but significant, elevation in body temperature by *Il-6* gene transfer (Fig. S1) suggests that an IL-6 mediated reduction in fat mass can be attributed to its action in stimulating thermogenesis and lipid utilization in BAT. Li et al. reported that an increase in central IL-6 levels stimulated the function of BAT and increased *Ucp1* expression and heat production [13]. Moreover, transplanted BAT controls mouse body composition and metabolism through an increase in circulating IL-6 [22], indicating that peripheral elevation of IL-6 is capable of exerting its beneficial role. In addition, hydrodynamic injection-mediated *Il-6* gene transfer further enhanced multiple thermogenic gene expression, including *Ucp*, *Pgc1 α* , *Pgc1 β* , *Cidea* and *Elovl3* (Fig. 7C). Furthermore, promotion of phosphorylated STAT3, a master molecule in the IL-6 signaling pathway and elevation of PGC-1 α and UCP1 proteins in BAT further confirm that IL-6 stimulated BAT function (Fig. 7D–F).

Different from BAT, WAT is the major organ in lipid storage. Sustained *Il-6* gene expression resulting from hydrodynamic gene transfer dramatically reduced epi-, sub-, and retro-WAT pad size (Fig. 2), suggesting that IL-6 promotes WAT lipolysis, which contributes to whole body weight loss. In fact, in vitro studies using 3T3-L1 pre-adipocytes and isolated human adipocytes have shown that IL-6

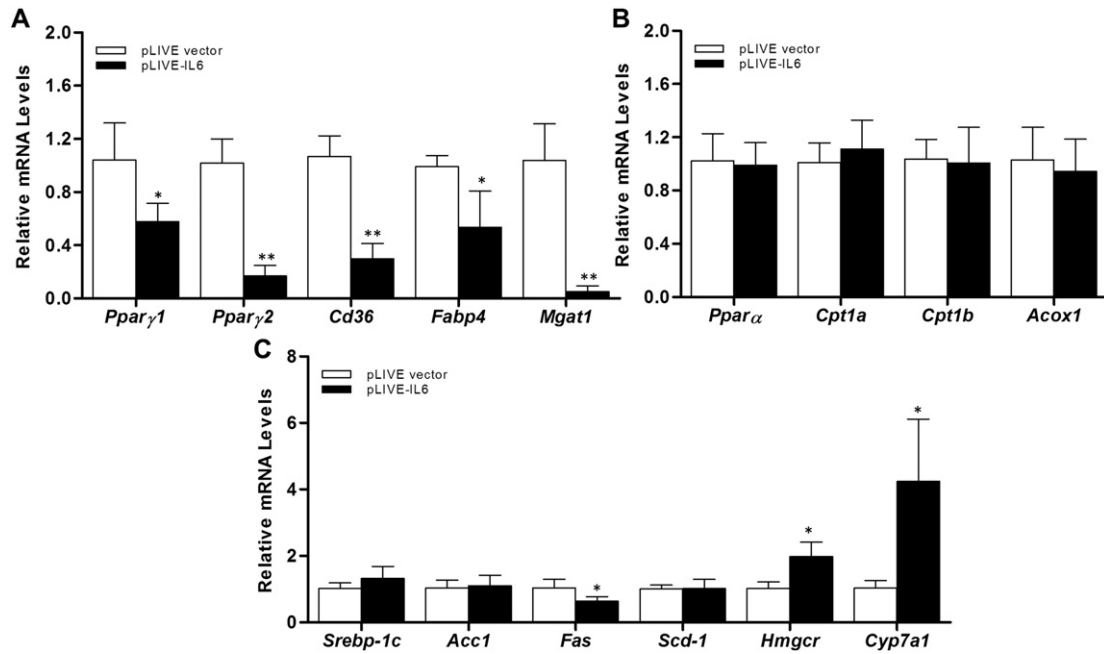


Fig. 5. Effect of *Il-6* gene transfer on hepatic lipid metabolism in obese mice. After HFD-feeding obese mice were sacrificed at the end of 6 weeks after gene transfer, total RNA from the liver was extracted and the relative mRNA levels of selected genes were analyzed by real time PCR. (A) Nuclear receptor genes for metabolic homeostasis, *Pparγ1*, *Pparγ2* and the target genes *Cd36*, *Fabp4* and *Mgat1*; (B) Genes involved in fatty acid oxidation, *Pparα*, *Cpt1a*, *Cpt1b* and *Acox1*; and (C) Genes involved in lipogenesis and cholesterol metabolism, *Srebp-1c*, *Acc1*, *Fas*, *Scd-1*, *Hmgcr* and *Cyp7a1*. Each data point represents the mean \pm SD (n = 4). *P < 0.05, **P < 0.01 compared to control group.

stimulates lipolysis and glycerol release [23,24]. In vivo human studies further prove that the infusion of recombinant IL-6 increased lipolysis and fat oxidation [25,26]. In line with these studies, our results show

that prolonged overexpression of the *Il-6* gene significantly enhances transcript levels of *Hsl* and *Atgl* in sub-WAT (Fig. 8A), the key enzymes involved in lipolysis. In the meantime, IL-6 also enhanced fatty acid

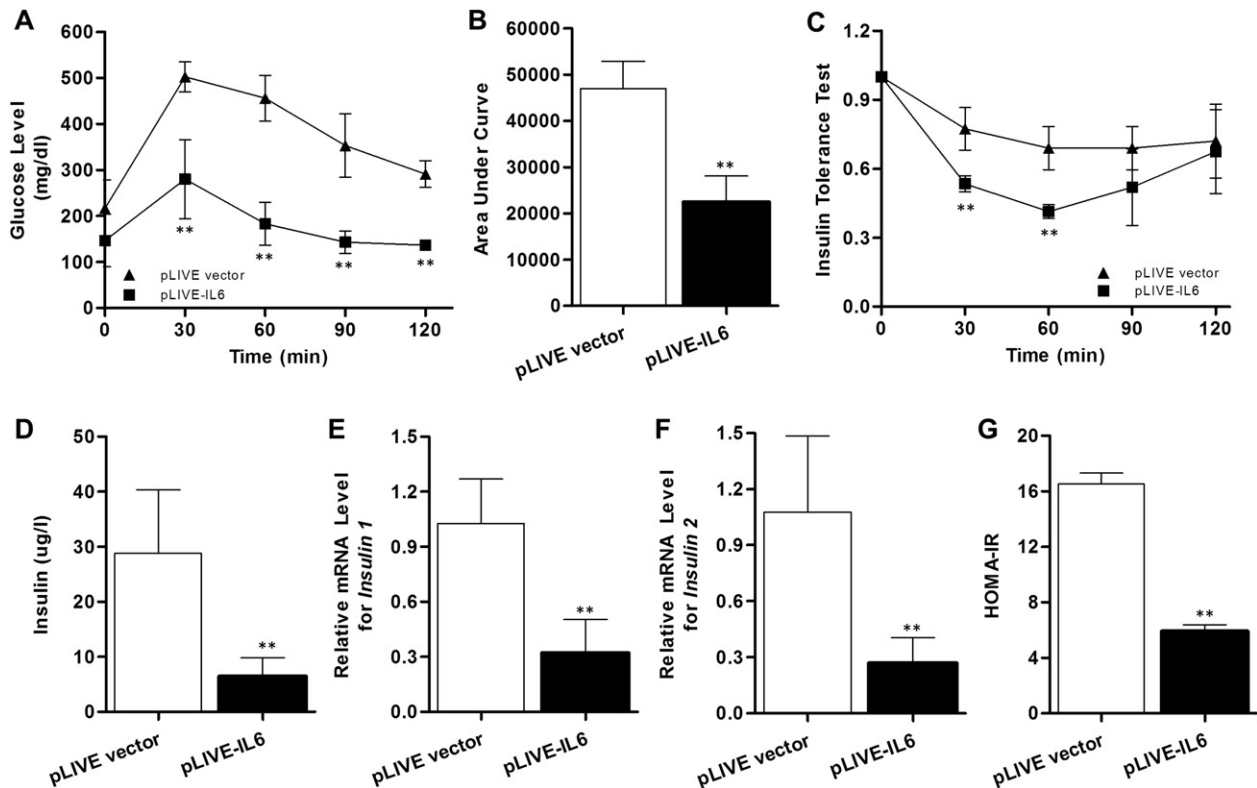


Fig. 6. IL-6 improves insulin sensitivity and glucose homeostasis in obese mice. (A) Time-dependent blood concentration of glucose upon *i.p.* injection of glucose (1.5 g/kg); (B) Area under the curve from glucose tolerance test; (C) Time-dependent ratio of glucose concentration upon *i.p.* injection of insulin (0.75 units/kg); (D) Insulin level at the end of 6 weeks after gene transfer; (E, F) mRNA levels of *insulin 1* and *insulin 2* in pancreas at the end of 6 weeks after gene transfer; (G) HOMA-IR values. Each data point represents the average \pm SD (n = 6). *P < 0.05, **P < 0.01 compared to control animals.

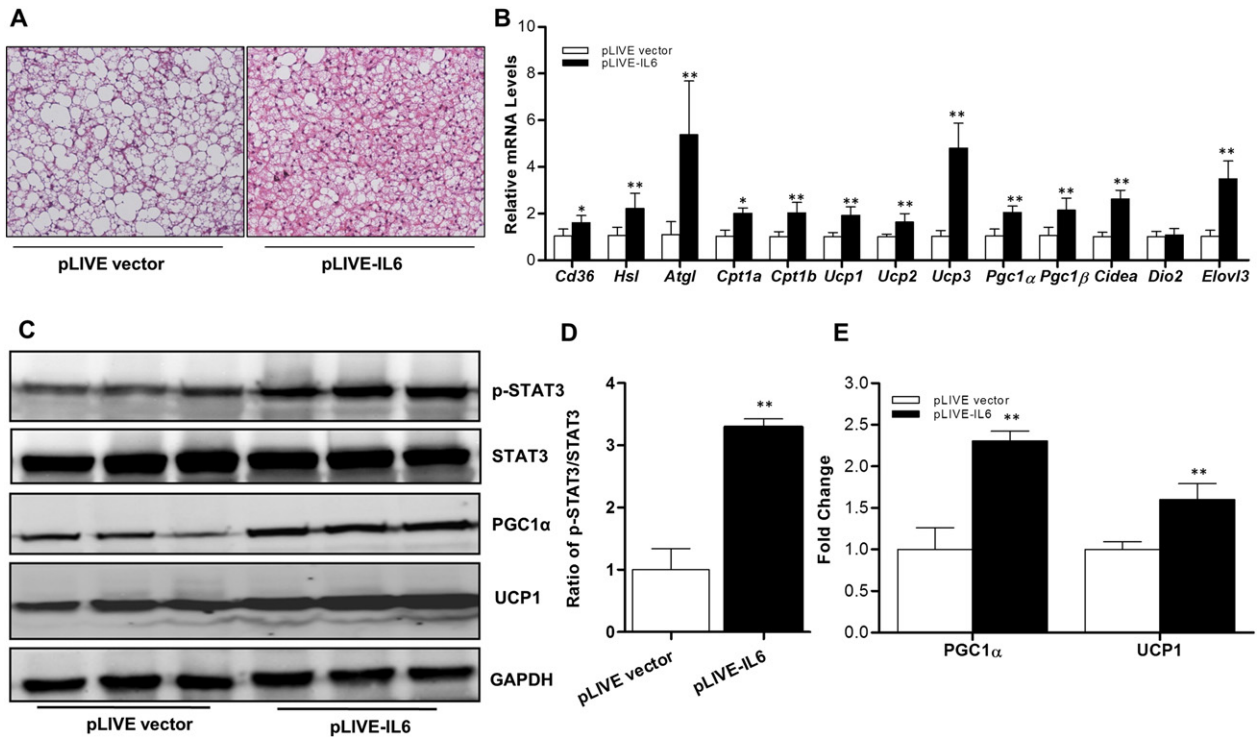


Fig. 7. *Il-6* gene transfer stimulated thermogenic activity in obese mice. (A) Representative images of H&E staining of BAT (200×); (B) Relative mRNA levels of genes involved in lipolysis, fatty acid β -oxidation or thermogenesis in BAT ($n = 4$); (C) Phosphorylation of STAT3, total STAT3, PGC1 α and UCP1 proteins in BAT determined by Western Blotting ($n = 3$); (D) Relative ratio of P-STAT3 to STAT3 based on the results of (C); (E) Change of PGC1 α and UCP1 protein level in BAT. Each data point represents the average \pm SD. * $P < 0.05$, ** $P < 0.01$ compared to control animals.

oxidation, as evidenced by increased mRNA levels of *Cpt1a* and *Cpt1b*. Moreover, IL-6 increased transcription of thermogenic genes in WAT (Figs. 8A, B), indicating its potential capability in WAT remodeling.

Skeletal muscle is an important organ involved in lipid metabolism. Therefore, we investigated the effect of *Il-6* gene transfer on lipid metabolism in skeletal muscle. A Western Blotting analysis showed that prolonged *Il-6* gene expression stimulated STAT3 and AMPK activation, consequently enhancing phosphorylation of ACC (Fig. 9A–D). AMPK is well documented to phosphorylate ACC, a rate-limiting step in the conversion of acetyl-CoA to malonyl-CoA. The phosphorylation of ACC inhibits its activity, leading to a decrease in malonyl-CoA and an increase in transferring long-chain fatty acyl-CoA into mitochondria for oxidation. In agreement with these results, other researchers also reported that short-term administration of IL-6 promotes lipid metabolism in rat and human skeletal muscle [27,28]. Overall, these results

demonstrate that sustained high levels of IL-6 resulting from hydrodynamic gene delivery stimulates lipolysis in WAT and promotes thermogenesis and lipid metabolism in BAT and skeletal muscle, consequently resulting in improvement of insulin resistance.

Several lines of studies have indicated that IL-6 exerts the protective role in various hepatic diseases. IL-6 stimulates liver regeneration and protects against liver injury [29,30]. Similarly, IL-6 is capable of correcting ethanol-induced hepatic steatosis in IL-6 deficient mice [31]. Moreover, 10 days of subcutaneous IL-6 injection ameliorates the fatty liver in genetic and diet-induced obese mice [32]. Concordance with these reports, *Il-6* gene transfer in our study dramatically reduced lipid accumulation as demonstrated by H&E and Oil Red O stained-liver sections and measured hepatic lipid levels (Fig. 4A–E). At the molecular level, IL-6 markedly suppressed mRNA levels of *Ppar γ* and their targeted genes including *Cd36*, *Fabp4* and *Mgat1* (Fig. 5A). PPAR γ plays an

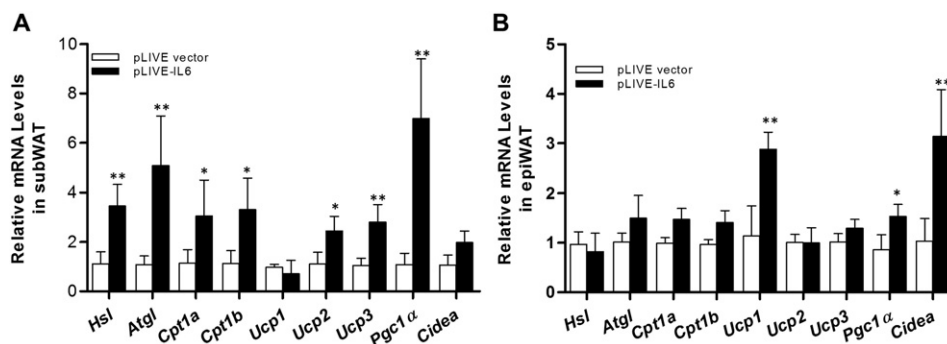


Fig. 8. IL-6 stimulates white adipocyte remodeling in obese mice. At the end of 6 weeks after gene delivery, mice were sacrificed. The mRNA level of genes involved in lipolysis and thermogenesis were determined in the subcutaneous (A) and epididymal (B) fat tissues by real time PCR. Each data point represents the average \pm SD of 4 animals in each group. * $P < 0.05$, ** $P < 0.01$ compared to control animals.

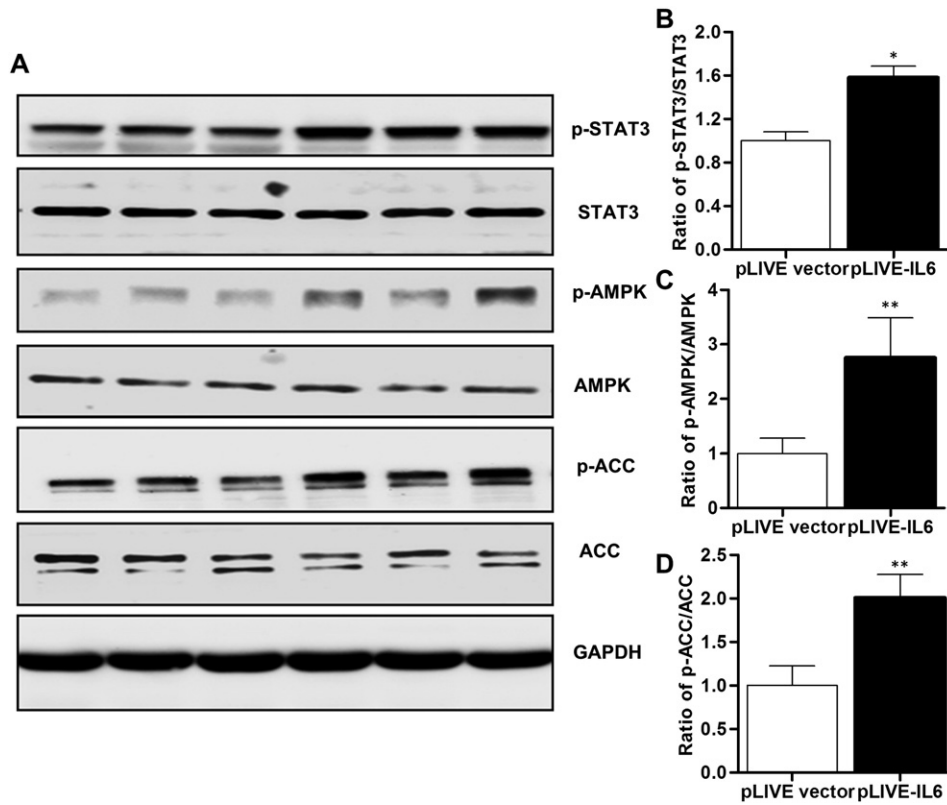


Fig. 9. Effect of IL-6 on fat oxidation in skeletal muscle of obese mice. After mice were sacrificed at the end of experiment, the gastrocnemius and soleus muscles were freshly collected and immediately frozen in liquid nitrogen, and then stored at -80°C . (A) Western Blotting analysis for total and phosphorylated STAT3, AMPK and ACC, as well as GAPDH; (B–D) The ratios of phosphorylated and the native forms of these proteins based on scanning image of (a). * $P < 0.05$, ** $P < 0.01$ compared to control group ($n = 3$).

important role in the development of hepatic steatosis. Overexpression of hepatic *Ppar γ* results in exacerbated liver steatosis [33]. Conversely, liver- and hepatocyte-specific *Ppar γ* knockout mice were protected against hepatic lipid accumulation [34–36]. Therefore, the inhibition of

hepatic *PPAR γ* pathway is responsible, at least in part, for its beneficial effect on hepatic steatosis. In addition, short-term IL-6 administration has been reported to increase hepatic *PPAR α* and fatty acid oxidation [32]. However, we did not see a change in

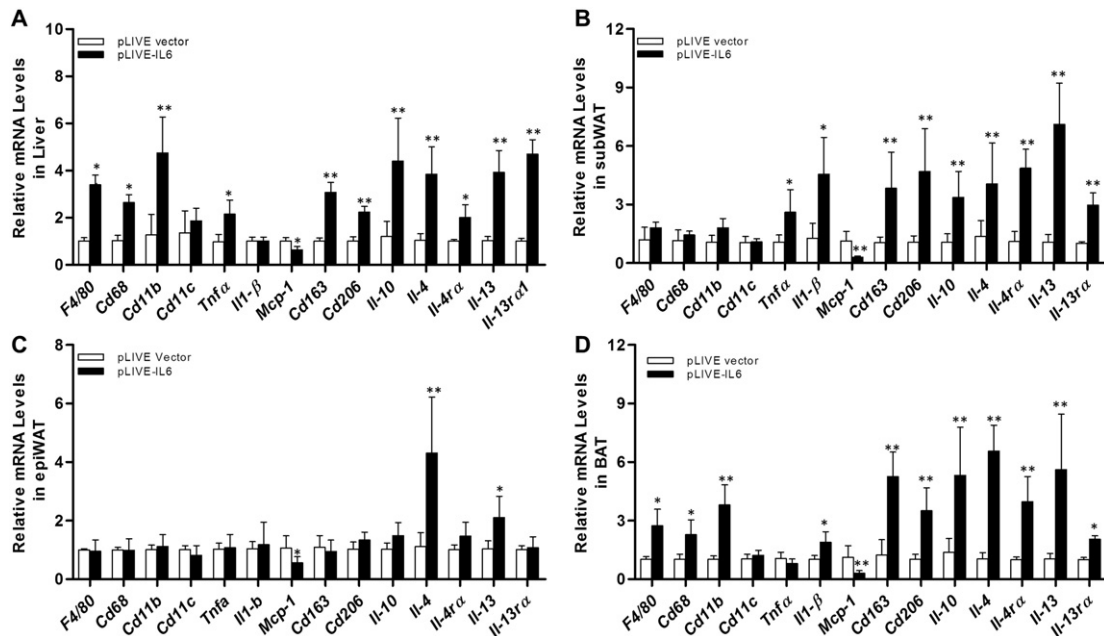


Fig. 10. Effect of *Il-6* gene transfer on mRNA levels of macrophage specific marker genes. Mice were sacrificed at the end of experiment. The liver, WAT and BAT tissues were collected and real time PCR was performed to detect mRNA levels of macrophage marker genes. General macrophage marker genes: *F4/80* and *Cd68*; M1-macrophage marker genes: *Cd11b*, *Cd11c*, *Tnf α* , *Il-1 β* , *Mcp-1*; and M2-macrophage marker genes, *Cd163*, *Cd206*, *Il-10*, *Il-4*, *Il-13*, and their receptor genes *Il-4 α* , *Il-13 α 1*. (A) liver; (B) subWAT; (C) epiWAT and (D) BAT. Each data point represents the average \pm SD of 4 animals in each group. * $P < 0.05$, ** $P < 0.01$ compared to control animals.

Pparα transcript levels and its target gene after the 6-week treatment (Fig. 5B), suggesting that activation of PPAR α is important for mediating short-term effects of IL-6, but may not be necessary for long-term IL-6 effects.

The role of IL-6 in insulin resistance remains debatable. Addition of IL-6 to HepG2 cells in culture and acute infusion of IL-6 in mice showed impaired insulin signaling and insulin sensitivity [37,38]. However, accumulating *in vivo* studies show the protective role of IL-6 in glucose homeostasis. IL-6 deficient mice and animals with hepatic disruption of IL-6 signaling pathway develop system insulin resistance [12,39]. Whereas IL-6 transgenic mice displayed higher sensitivity to insulin [10]. In our study, *Il-6* gene transfer greatly repressed diet-induced hyperglycemia and hyperinsulinemia. IL-6 quickly reduced obesity-induced high blood glucose levels and consistently kept it at normal levels throughout the experiment. IL-6 evidently enhanced insulin sensitivity, as reflected by GTT, ITT and reduced HOMA-IR (Fig. 6A–C). Accordingly, obesity-induced hyperinsulinemia and increased expression of pancreatic insulin genes were dramatically reduced (Fig. 6D–F). Similarly, reduction in adiposity and enhanced lipid utilization by *Il-6* overexpression also improve glucose homeostasis. In addition, a recent study has shown that IL-6 is capable of stimulating glucagon-like peptide-1 secretion from L cells and alpha cells, enhancing insulin secretion and reaction [40], which may also contribute to the beneficial effect of IL-6 on glucose metabolism. Taken together, our study supports the notion that IL-6 alleviates obesity-related insulin resistance and improved glucose homeostasis.

Macrophage infiltration is a common feature in HFD-induced obesity. A previous study shows that HFD induces a shift of macrophage phenotype from a M2-polarized state in lean animals to a M1 pro-inflammatory state, characterized by high mRNA level of marker gene such as *F4/80* and *CD11c*, and higher level of pro-inflammatory cytokines [41]. Our results show that IL-6 did not reduce the macrophage infiltration. However, IL-6 markedly enhanced M2 macrophage phenotype, as evidenced by higher mRNA levels of *Cd163* and *Cd206*, anti-inflammatory factor *Il-10*, stimulator *Il-4*, *Il-13* and their receptor genes (Fig. 10A–D). M2 macrophages are generally associated with tissue surveillance and enhanced sensitivity to insulin. Recent studies reported that type 2 cytokines, such as IL-4 and IL-13, and alternatively activated macrophages are involved in adaptive thermogenesis and beige cell production, suggesting the important and beneficial role of M2 macrophages in obesity [42–44]. In line with our study, Mauer et al. [45] have shown that a conditionally inactivated IL-6 receptor α in myeloid cells increased systemic inflammation, while administration of IL-6 enhanced IL-4 receptor expression and promoted IL-4 mediated alternative activation of macrophages, which consequently limited obesity-associated chronic inflammation and insulin resistance, as well as LPS-stimulated endotoxemia. Overall, our data suggest that IL-6 treatment in obese mice counterbalances the obesity-related pro-inflammation by elevation of M2 phenotype of macrophages.

In summary, results presented in this study demonstrate that sustained *Il-6* gene expression in obese mice, achieved by hydrodynamic gene delivery, enhances lipolysis and thermogenesis, and consequently induces weight loss and diminishes obesity-related fatty liver and insulin resistance. These findings provide direct evidence in support of the potential health benefits of IL-6 in managing obesity and obesity-associated metabolic disorders. Evidently, additional efforts are needed to define the factors that are possibly involved in the process. Additional studies are also needed to assess the potential side effects that IL-6 may induce due to its function as a pro-inflammatory cytokine. Considering the relative smaller BAT depots in human and the difference between mice and human in energy metabolism and thermogenesis, caution should be taken when applying the presented results to humans.

Supplementary data to this article can be found online at <http://dx.doi.org/10.1016/j.bbadis.2015.01.017>.

Conflict of interest

The authors declared no conflict of interest.

Acknowledgements

We would like to thank Ms. Ryan Fugett for English editing. The study was supported in part by grants from the National Institutes of Health (RO1EB007357 and RO1HL098295).

References

- [1] H. Tilg, E. Trehu, M.B. Atkins, C.A. Dinarello, J.W. Mier, Interleukin-6 (IL-6) as an anti-inflammatory cytokine: induction of circulating IL-1 receptor antagonist and soluble tumor necrosis factor receptor p55, *Blood* 83 (1994) 113–118.
- [2] J.S. Stumhofer, J.S. Silver, A. Laurence, P.M. Porrett, T.H. Harris, L.A. Turka, M. Ernst, C.J. Saris, J.J. O'Shea, C.A. Hunter, Interleukins 27 and 6 induce STAT3-mediated T cell production of interleukin 10, *Nat. Immunol.* 8 (2007) 1363–1371.
- [3] R. Starkie, S.R. Ostrowski, S. Jauffred, M. Febbraio, B.K. Pedersen, Exercise and IL-6 infusion inhibit endotoxin-induced TNF- α production in humans, *FASEB J.* 17 (2003) 884–886.
- [4] V. Wallenius, K. Wallenius, B. Ahren, M. Rudling, H. Carlsten, S.L. Dickson, C. Ohlsson, J.O. Jansson, Interleukin-6-deficient mice develop mature-onset obesity, *Nat. Med.* 8 (2002) 75–79.
- [5] M.E. Trujillo, S. Sullivan, I. Harten, S.H. Schneider, A.S. Greenberg, S.K. Fried, Interleukin-6 regulates human adipose tissue lipid metabolism and leptin production *in vitro*, *J. Clin. Endocrinol. Metab.* 89 (2004) 5577–5582.
- [6] I. Wernstedt, B. Olsson, M. Jernas, S. Paglialunga, L.M. Carlsson, U. Smith, K. Cianflone, K. Wallenius, V. Wallenius, Increased levels of acylation-stimulating protein in interleukin-6-deficient (IL-6 $^{-/-}$) mice, *Endocrinology* 147 (2006) 2690–2695.
- [7] J.C. Pickup, M.B. Mattock, G.D. Chusney, D. Burt, NIDDM as a disease of the innate immune system: association of acute-phase reactants and interleukin-6 with metabolic syndrome X, *Diabetologia* 40 (1997) 1286–1292.
- [8] A.D. Pradhan, J.E. Manson, N. Rifai, J.E. Buring, P.M. Ridker, C-reactive protein, interleukin 6, and risk of developing type 2 diabetes mellitus, *J. Am. Med. Assoc.* 286 (2001) 327–334.
- [9] B. Vozarova, C. Weyer, K. Hanson, P.A. Tataranni, C. Bogardus, R.E. Pratley, Circulating interleukin-6 in relation to adiposity, insulin action, and insulin secretion, *Obes. Res.* 9 (2001) 414–417.
- [10] K. Ostrowski, P. Schjerling, B.K. Pedersen, Physical activity and plasma interleukin-6 in humans – effect of intensity of exercise, *Eur. J. Appl. Physiol.* 83 (2000) 512–515.
- [11] J.W. Helge, B. Stallknecht, B.K. Pedersen, H. Galbo, B. Kiens, E.A. Richter, The effect of graded exercise on IL-6 release and glucose uptake in human skeletal muscle, *J. Physiol.* 546 (2003) 299–305.
- [12] V.B. Matthews, T.L. Allen, S. Risis, M.H. Chan, D.C. Henstridge, N. Watson, L.A. Zaffino, J.R. Babb, J. Boon, P.J. Meikle, J.B. Jowett, M.J. Watt, J.O. Jansson, C.R. Bruce, M.A. Febbraio, Interleukin-6-deficient mice develop hepatic inflammation and systemic insulin resistance, *Diabetologia* 53 (2010) 2431–2441.
- [13] G. Li, R.L. Klein, M. Matheny, M.A. King, E.M. Meyer, P.J. Scarpace, Induction of uncoupling protein 1 by central interleukin-6 gene delivery is dependent on sympathetic innervation of brown adipose tissue and underlies one mechanism of body weight reduction in rats, *Neuroscience* 115 (2002) 879–889.
- [14] M. Sadagurski, L. Norquay, J. Farhang, K. D'Aquino, K. Copps, M.F. White, Human IL6 enhances leptin action in mice, *Diabetologia* 53 (2010) 525–535.
- [15] K. Wallenius, V. Wallenius, D. Sunter, S.L. Dickson, J.O. Jansson, Intracerebroventricular interleukin-6 treatment decreases body fat in rats, *Biochem. Biophys. Res. Commun.* 293 (2002) 560–565.
- [16] H. Mukumoto, Y. Takahashi, M. Ando, M. Nishikawa, Y. Takakura, Expression profile-dependent improvement of insulin sensitivity by gene delivery of interleukin-6 in a mouse model of type II diabetes, *Mol. Pharm.* 10 (2013) 3812–3821.
- [17] F. Liu, Y. Song, D. Liu, Hydrodynamics-based transfection in animals by systemic administration of plasmid DNA, *Gene Ther.* 6 (1999) 1258–1266.
- [18] Y. Ma, D. Liu, Hydrodynamic delivery of adiponectin and adiponectin receptor 2 gene blocks high-fat diet-induced obesity and insulin resistance, *Gene Ther.* 20 (2013) 846–852.
- [19] Y. Ma, Y. Huang, L. Yan, M. Gao, D. Liu, Synthetic FXR agonist GW4064 prevents diet-induced hepatic steatosis and insulin resistance, *Pharm. Res.* 30 (2013) 1447–1457.
- [20] Y. Ma, M. Gao, D. Liu, Chlorogenic acid improves high fat diet-induced hepatic steatosis and insulin resistance in mice, *Pharm. Res.* (2014), <http://dx.doi.org/10.1007/s11095-014-1526-9>.
- [21] C.A. Dinarello, J.G. Cannon, J. Mancilla, I. Bishai, J. Lees, F. Cocceani, Interleukin-6 as an endogenous pyrogen – induction of prostaglandin-E2 in brain but not in peripheral-blood mononuclear-cells, *Brain Res.* 562 (1991) 199–206.
- [22] K.I. Stanford, R.J.W. Middelbeek, K.L. Townsend, D. An, E.B. Nygaard, K.M. Hitchcox, K.R. Markan, K. Nakano, M.F. Hirshman, Y.H. Tseng, L.J. Goodyear, Brown adipose tissue regulates glucose homeostasis and insulin sensitivity, *J. Clin. Invest.* 123 (2013) 215–223.
- [23] A.S. Greenberg, R.P. Nordan, J. McIntosh, J.C. Calvo, R.O. Scow, D. Jablons, Interleukin 6 reduces lipoprotein lipase activity in adipose tissue of mice *in vivo* and in 3T3-L1 adipocytes: a possible role for interleukin 6 in cancer cachexia, *Cancer Res.* 52 (1992) 4113–4116.

- [24] G. Path, S.R. Bornstein, M. Gurniak, G.P. Chrousos, W.A. Scherbaum, H. Hauner, Human breast adipocytes express interleukin-6 (IL-6) and its receptor system: increased IL-6 production by beta-adrenergic activation and effects of IL-6 on adipocyte function, *J. Clin. Endocrinol. Metab.* 86 (2001) 2281–2288.
- [25] G. van Hall, A. Steensberg, M. Sacchetti, C. Fischer, C. Keller, P. Schjerling, N. Hiscock, K. Moller, B. Saltin, M.A. Febbraio, B.K. Pedersen, Interleukin-6 stimulates lipolysis and fat oxidation in humans, *J. Clin. Endocrinol. Metab.* 88 (2003) 3005–3010.
- [26] E.W. Petersen, A.L. Carey, M. Sacchetti, G.R. Steinberg, S.L. Macaulay, M.A. Febbraio, B.K. Pedersen, Acute IL-6 treatment increases fatty acid turnover in elderly humans in vivo and in tissue culture in vitro, *Am. J. Physiol. Endocrinol. Metab.* 288 (2005) E155–E162.
- [27] M. Kelly, M.S. Gauthier, A.K. Saha, N.B. Ruderman, Activation of AMP-activated protein kinase by interleukin-6 in rat skeletal muscle: association with changes in cAMP, energy state, and endogenous fuel mobilization, *Diabetes* 58 (2009) 1953–1960.
- [28] E. Wolsk, H. Mygind, T.S. Grondahl, B.K. Pedersen, G. van Hall, IL-6 selectively stimulates fat metabolism in human skeletal muscle, *Am. J. Physiol. Endocrinol. Metab.* 299 (2010) E832–E840.
- [29] D.E. Cressman, L.E. Greenbaum, R.A. DeAngelis, G. Ciliberto, E.E. Furth, V. Poli, R. Taub, Liver failure and defective hepatocyte regeneration in interleukin-6-deficient mice, *Science* 274 (1996) 1379–1383.
- [30] T.A. Zimmers, I.H. McKillop, R.H. Pierce, J.Y. Yoo, L.G. Koniaris, Massive liver growth in mice induced by systemic interleukin 6 administration, *Hepatology* 38 (2003) 326–334.
- [31] O. El-Assal, F. Hong, W.H. Kim, S. Radaeva, B. Gao, IL-6-deficient mice are susceptible to ethanol-induced hepatic steatosis: IL-6 protects against ethanol-induced oxidative stress and mitochondrial permeability transition in the liver, *Cell. Mol. Immunol.* 1 (2004) 205–211.
- [32] F. Hong, S. Radaeva, H.N. Pan, Z.C. Tian, R. Veech, B. Gao, Interleukin 6 alleviates hepatic steatosis and ischemia/reperfusion injury in mice with fatty liver disease, *Hepatology* 40 (2004) 933–941.
- [33] S.T. Yu, K. Matsusue, P. Kashireddy, W.Q. Cao, V. Yeldandi, A.V. Yeldandi, M.S. Rao, F.J. Gonzalez, J.K. Reddy, Adipocyte-specific gene expression and adipogenic steatosis in the mouse liver due to peroxisome proliferator-activated receptor gamma 1 (PPAR gamma 1) overexpression, *J. Biol. Chem.* 278 (2003) 498–505.
- [34] O. Gavrilova, M. Haluzik, K. Matsusue, J.J. Cutson, L. Johnson, K.R. Dietz, C.J. Nicol, C. Vinson, F.J. Gonzalez, M.L. Reitman, Liver peroxisome proliferator-activated receptor gamma contributes to hepatic steatosis, triglyceride clearance, and regulation of body fat mass, *J. Biol. Chem.* 278 (2003) 34268–34276.
- [35] K. Matsusue, M. Haluzik, G. Lambert, S.H. Yim, O. Gavrilova, J.M. Ward, B. Brewer Jr., M.L. Reitman, F.J. Gonzalez, Liver-specific disruption of PPARgamma in leptin-deficient mice improves fatty liver but aggravates diabetic phenotypes, *J. Clin. Invest.* 111 (2003) 737–747.
- [36] E. Moran-Salvador, M. Lopez-Parra, V. Garcia-Alonso, E. Titos, M. Martinez-Clemente, A. Gonzalez-Periz, C. Lopez-Vicario, Y. Barak, V. Arroyo, J. Claria, Role for PPAR gamma in obesity-induced hepatic steatosis as determined by hepatocyte- and macrophage-specific conditional knockouts, *FASEB J.* 25 (2011) 2538–2550.
- [37] J.J. Senn, P.J. Klover, I.A. Nowak, R.A. Mooney, Interleukin-6 induces cellular insulin resistance in hepatocytes, *Diabetes* 51 (2002) 3391–3399.
- [38] H.J. Kim, T. Higashimori, S.Y. Park, H. Choi, J.Y. Dong, Y.J. Kim, H.L. Noh, Y.R. Cho, G. Cline, Y.B. Kim, J.K. Kim, Differential effects of interleukin-6 and -10 on skeletal muscle and liver insulin action in vivo, *Diabetes* 53 (2004) 1060–1067.
- [39] F.T. Wunderlich, P. Strohle, A.C. Konner, S. Gruber, S. Tovar, H.S. Bronneke, L. Juntti-Berggren, L.S. Li, N. van Rooijen, C. Libert, P.O. Berggren, J.C. Bruning, Interleukin-6 Signaling in liver-parenchymal cells suppresses hepatic inflammation and improves systemic insulin action, *Cell Metab.* 12 (2010) 237–249.
- [40] H. Ellingsgaard, I. Hauselmann, B. Schuler, A.M. Habib, L.L. Baggio, D.T. Meier, E. Eppler, K. Bouzakri, S. Wueest, Y.D. Muller, A.M.K. Hansen, M. Reinecke, D. Konrad, M. Gassmann, F. Reimann, P.A. Halban, J. Gromada, D.J. Drucker, F.M. Gribble, J.A. Ehres, M.Y. Donath, Interleukin-6 enhances insulin secretion by increasing glucagon-like peptide-1 secretion from L cells and alpha cells, *Nat. Med.* 17 (2011) 1481–U1500.
- [41] C.N. Lumeng, J.L. Bodzin, A.R. Saltiel, Obesity induces a phenotypic switch in adipose tissue macrophage polarization, *J. Clin. Invest.* 117 (2007) 175–184.
- [42] R.R. Rao, J.Z. Long, J.P. White, K.J. Svensson, J. Lou, I. Lokurkar, M.P. Jedrychowski, J.L. Ruas, C.D. Wrann, J.C. Lo, D.M. Camera, J. Lachey, S. Gygi, J. Seehra, J.A. Hawley, B.M. Spiegelman, Meteorin-like is a hormone that regulates immune-adipose interactions to increase beige fat thermogenesis, *Cell* 157 (2014) 1279–1291.
- [43] Y. Qiu, K.D. Nguyen, J.I. Odegaard, X. Cui, X. Tian, R.M. Locksley, R.D. Palmiter, A. Chawla, Eosinophils and type 2 cytokine signaling in macrophages orchestrate development of functional beige fat, *Cell* 157 (2014) 1292–1308.
- [44] K.D. Nguyen, Y. Qiu, X. Cui, Y.P. Goh, J. Mwangi, T. David, L. Mukundan, F. Brombacher, R.M. Locksley, A. Chawla, Alternatively activated macrophages produce catecholamines to sustain adaptive thermogenesis, *Nature* 480 (2011) 104–108.
- [45] J. Mauer, B. Chaurasia, J. Goldau, M.C. Vogt, J. Ruud, K.D. Nguyen, S. Theurich, A.C. Hausen, J. Schmitz, H.S. Bronneke, E. Estevez, T.L. Allen, A. Mesaros, L. Partridge, M.A. Febbraio, A. Chawla, F.T. Wunderlich, J.C. Bruning, Signaling by IL-6 promotes alternative activation of macrophages to limit endotoxemia and obesity-associated resistance to insulin, *Nat. Med.* 15 (2014) 423–430.